Differential cross sections for positron-xenon elastic scattering

J. P. Marler* and C. M. Surko
Department of Physics, University of California, San Diego, California 92093-0319, USA

R. P. McEachran
Centre for Antimatter-Matter Studies, Research School of Physical Sciences and Engineering, Australian National University, ACT 0200, Australia

A. D. Stauffer
Department of Physics, York University, Toronto, Ontario, Canada M3J 1P3

(Received 8 April 2006; published 8 June 2006)

Absolute measurements of differential cross sections for the elastic scattering of positrons from xenon are made at 2, 5 and 8 eV using a trap-based beam and the technique of measuring scattering cross sections in a strong magnetic field. Calculations are carried out using the relativistic Dirac equations with a static plus polarization potential. Generally good absolute agreement is found between experiment and theory.

DOI: 10.1103/PhysRevA.73.064702 PACS number(s): 34.85.+x

Experimental studies of positron scattering from atoms and molecules have lagged behind electron scattering because of the difficulties involved in creating sufficiently monoenergetic and intense beams of positrons to carry out such measurements. However, with the recent development of efficient positron traps and trap-based cold beams and techniques to study scattering in a magnetic field [1–3], it is now possible to make measurements of interest that were not possible previously. In this paper, absolute measurements are reported for the differential cross sections (DCS) for elastic scattering of positrons from xenon atoms at 2, 5 and 8 eV. Where comparisons are available (i.e., at 5 eV [4]), the data presented here agree reasonably well with those published previously. However, the data presented here improve upon the previous measurements in three ways. The present measurements provide absolute, as opposed to relative cross section measurements. In addition, they are made over a larger range of near-forward scattering angles and include data at smaller values of incident positron energy.

From a theoretical point of view, the scattering of positrons has been treated by and large as the scattering of an electron with positive charge. However, there are two significant differences between electron and positron scattering. Since the positron is a distinct particle, there is no exchange reaction between the incident positron and the bound atomic electrons. This leads to a simplification over electron scattering. On the other hand, the formation of a positronium (Ps) atom (the bound state of an electron and positron pair) is possible and is typically the inelastic channel with the lowest threshold. This threshold is equal to the ionization energy of the atom minus the binding energy of a positronium atom, namely half a Rydberg, 6.8 eV.

Ps formation is difficult to treat theoretically since it is a two-center problem with one center the nucleus of the atom and the other at the center of mass of the positronium atom. Since positronium is a light system, semiclassical methods are not applicable. For xenon, the Ps formation threshold is at 5.33 eV. Thus the measurements presented here at 2 eV are well below this threshold; the ones at 5 eV are very close to this threshold, where the effects of the closed positronium channels can induce resonant behavior; and the ones at 8 eV are well above the threshold, where this inelastic channel is open though the channels for electronic excitation of the atom are still closed. Due to the fact that xenon is a heavy atom, the calculations are carried out within a framework of the Dirac equations using the *j-j* coupling representation (i.e., rather than the Schrödinger equation using *LS* coupling).

The experimental technique for forming a cold, trap-based positron beam has been described in detail previously [1,5]. Positrons from a ^{22}Na radioactive source and neon moderator are trapped and cooled in a three-stage buffer-gas Penning-Malmberg trap in a 0.15 T magnetic field. The positrons cool to the temperature of the buffer gas and surrounding electrodes (i.e., 300 K≡25 meV). Once cooled, positron bunches are pushed out of the third stage of the trap, as illustrated in Fig. 1, and magnetically guided through a scattering cell and then through a retarding potential analyzer (RPA). The RPA is used to analyze the incident energy dis-

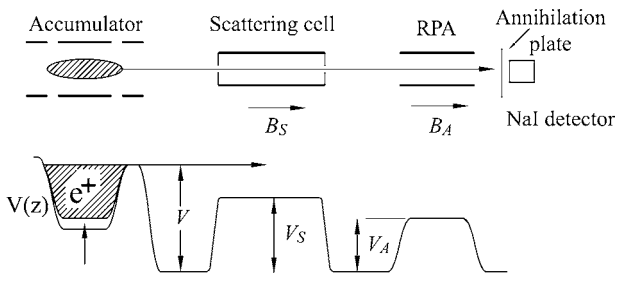

FIG. 1. Schematic diagram of the electrode structure (above) and the electric potentials (below) used to study scattering with a trap-based positron beam. The positron beam is guided by an applied magnetic field of strength 0.09 T through the scattering cell and the retarding potential analyzer (RPA).

*Current address: Department of Physics, Lawrence University, Appleton, WI 54911.

tribution of the beam (i.e., with the test gas removed from the scattering cell). The energy resolution of the positron beam used in the experiments described here is ~25 meV (full width at half maximum).

The cross section measurements presented here were done using a technique that relies on the fact that the positron orbits are strongly magnetized [2,3]. In a strong magnetic field, namely where the positron's gyroradius is small compared to the characteristic dimensions of the scattering apparatus but still large compared to atomic dimensions, the total kinetic energy is separable into two components: energy in motion parallel to the magnetic field, $E_{\parallel}$, and that in the cyclotron motion in the direction perpendicular to the field, $E_{\perp}$.

If a positron is scattered in the gas cell, then some of the energy of the positron will be transferred from the parallel to the perpendicular component, with the specific amount depending on the scattering angle, (θ). In the case where only elastic scattering is present, energy is conserved, and $E=E'=E'_{\parallel}+E'_{\perp}$ (where $'$ indicates the final value). In this case, θ is related to the incident energy, E, and final parallel energy, $E'_{\parallel}$, by [3]

$$E'_{\parallel} = E\cos^2\theta. \tag{1}$$

The RPA measures only the final parallel energy of the positron. Therefore making a measurement of positron throughput as a function of $E_{\parallel}$ (as determined by raising the applied voltage on the RPA) determines the differential cross section. Thus, absolute cross sections are obtained by normalizing the transmitted signal to the incident beam strength using the measured target-gas density and path length. Absolute measurements of the cross section can be obtained without an absolute measurement of the initial beam current. The gas cell used in these experiments had small entrance and exit apertures (0.5 cm in diameter), and so the pressure and path length can be determined to a high degree of accuracy [3]. There is an uncertainty in path length introduced by scattering at an angle. For the measurements reported here, this effect produces ~10% overestimate of the cross section [3], which is neglected for the data reported here.

If the energy of the incoming positron is greater than the lowest inelastic threshold, then Eq. (1) is no longer valid. A decrease in $E'_{\parallel}$ may be the result of a combination of loss of initial energy to the perpendicular direction and loss of energy to the atom of molecule. This sets an upper limit as to the highest incident energy that can be studied without resorting to other means [3]. The first excited electronic state in Xe has a threshold of 8.32 eV which is above the range of positron energies considered here. Positronium formation is also not relevant, but for a different reason. It results in a loss of positrons from the beam. Thus it is possible to account for this loss directly by measuring the strength of the beam with the test gas in the cell and the RPA grounded.

In the current apparatus, positrons that are scattered in the backward direction are reflected off the exit gate of the three-stage trap and then retransmitted to the collector plate. Due to this effect, the measured DCS are "folded" around 90°, with the angles $\theta°$ and $(180-\theta)°$ summed. As a consequence, below, the measurements are compared with the theoretical predictions for this same sum.

The scattering of positrons by xenon is treated as a potential scattering problem, where the potential includes the static potential of the unperturbed atom plus a polarization potential [6] representing the perturbation of the atomic charge distribution by the incoming positron. Note that the static potential for a positron in the field of an atom has the opposite sign to that for an electron, but the polarization potential has the same sign to first order for both projectiles.

Since xenon is a heavy atom, it is better represented in *j-j* coupling rather than *LS* coupling. Thus the static potential is calculated using Dirac-Fock wave functions produced by the multi-configuration Dirac-Fock program [7]. The polarization potential is calculated nonrelativistically, since its effect is only appreciable at large distances where the relativistic effects of the large nuclear charge are screened by the atomic electrons.

The Dirac equations

$$\frac{d}{dr}f_\kappa(r) + \frac{\kappa}{r}f_\kappa(r) - \alpha\left[\frac{2}{\alpha^2} - V(r) + \epsilon\right]g_\kappa(r) = 0 \tag{2}$$

$$\frac{d}{dr}g_\kappa(r) - \frac{\kappa}{r}g_\kappa(r) + \alpha[-V(r) + \epsilon]f_\kappa(r) = 0 \tag{3}$$

are used to determine the scattering wave function. Here f_κ and g_κ are the large and small radial components of the scattered wave function with quantum number κ where

$$j = |\kappa| - 1/2 \tag{4}$$

$$l = \begin{cases} \kappa & \text{if } \kappa > 0 \\ -\kappa - 1 & \text{if } \kappa < 0 \end{cases} \tag{5}$$

and j is the total angular momentum of the incident positron and l is its orbital angular momentum. $V(r)$ is the sum of the static and polarization potentials while α is the fine-structure constant and ϵ is the kinetic energy of the positron. Asymptotically

$$f_\kappa(r) \underset{r\to\infty}{\approx} \sin\left(kr - \frac{l\pi}{2} - \delta_\kappa\right), \tag{6}$$

where k is the linear momentum of the positron and δ_κ is the phase shift. The DCS are calculated from the phase shifts.

The experimental and theoretical results for positron scattering from xenon are shown in Figs. 2–4. The dashed curves are the calculated DCS. Because the experiment cannot distinguish between positrons scattered in the forward and backward directions, the full curves represent the sum of the calculated DCS at scattering angles θ and $\pi-\theta$.

At 2 eV there is very good agreement between the measurements and the calculated values except at small scattering angles. At 5 and 8 eV, where the effects of positronium formation could be significant, the agreement is less good although the magnitudes and dependence on energy of the predictions and measurements are very similar. Also shown in Figs. 2 and 3 are the corresponding electron data of Ref. [8] at 1.75 and 4.75 eV, respectively. It is interesting to note

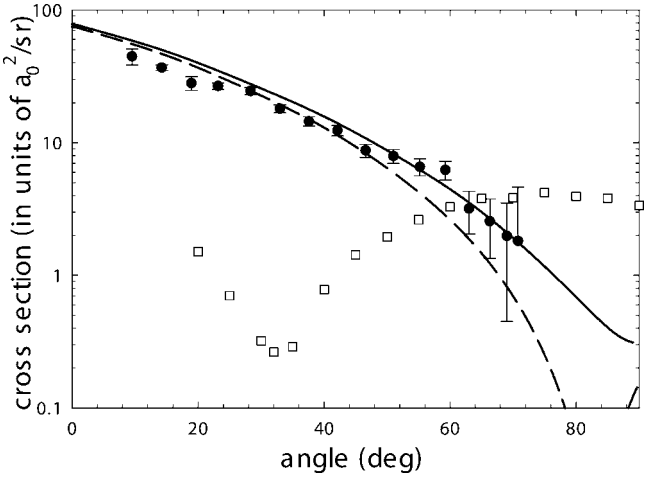

FIG. 2. (●) Absolute differential cross section measurements for elastic scattering of positrons from xenon at an incident energy of 2 eV, in units of a_o^2/sr, where a_o is the Bohr radius; (--) absolute theoretical prediction for this cross section from the present calculations, with no fitted parameters; and (—) the theoretical prediction folded about 90°, which is the appropriate comparison with the measurements. Also shown for comparison (□) are the electron-impact data of Ref. [8].

that the magnitude of both the electron and positron differential cross sections are comparable at these energies although for entirely different reasons.

In general, electron cross sections are much larger than the corresponding positron cross sections at low energies due to the deeper penetration of the electron into the atomic charge cloud. However, in the case of xenon there is a broad Ramsauer minimum either side of 0.8–0.9 eV caused by the *s*- and *p*-wave phase shifts passing through zero. At 1.75 eV the electron *p*-wave phase shifts are much smaller than the *d*-wave phase shifts and comparable with the *f*-wave phase shifts. This, in turn, gives rise to the minimum in the electron

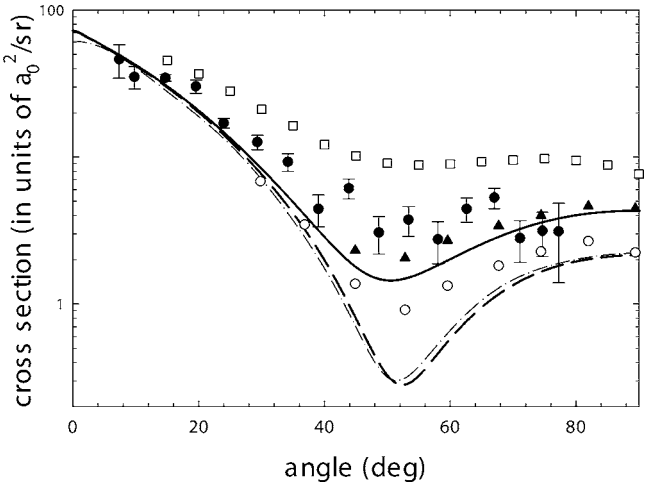

FIG. 3. Same as Fig. 2 but at an incident positron energy of 5 eV. Also shown are experimental data (○) of [4] and (▲) an estimate of those data folded about 90° for comparison with the current data. The dot-dashed line is the result of the previous, nonrelativistic polarized orbital calculation [6].

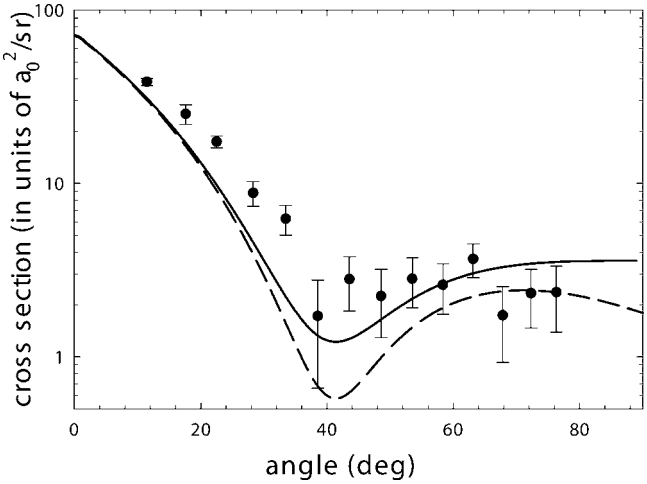

FIG. 4. Same as Fig. 2 but at an incident positron energy of 8 eV.

DCS around 35°. On the other hand, the shape of the positron DCS at this energy is dominated by the *p*-wave phase shifts which, in turn, gives rise to a minimum around 90°. At 4.75 eV the shape of the DCS for both electrons and positrons is influenced primarily by the *p*- and *d*-wave phase shifts and hence in both cases the minimum in the respective differential cross sections occurs around 55°.

Shown in Fig. 3 for the data at 5 eV are the predictions of the nonrelativistic polarized orbital calculation of Ref. [6]. As indicated in the figure, the differences between the predictions of this theory, which uses *LS* coupling, and the present, relativistic treatment using *j-j* coupling are relatively minor. The corresponding difference between a nonrelativistic and a relativistic treatment for electron scattering is much larger due to the exchange interaction [9]. Also shown for comparison in Fig. 3 are measurements from Ref. [4]. To obtain absolute values, the authors of Ref. [4] normalized their data to the nonrelativistic polarized orbital calculation of Ref. [6]. The agreement between the two sets of experimental data is reasonably good over the range of overlap.

Results are reported here for the absolute differential cross sections for positron scattering from xenon at 2, 5, and 8 eV including near-forward scattering angles as small as 15°. The agreement with relativistic calculations using a polarization potential is very satisfactory as is the comparison with previous measurements in the range of angles and energies where other data are available. It would be of interest to investigate whether inclusion of positronium formation in the theory would further improve this agreement at energies $\geqslant$5 eV.

We wish to thank S. J. Buckman for suggesting the experimental measurements and for helpful conversations, J. P. Sullivan for helpful conversations, and G. Jerzewski for his expert technical assistance. The work at UCSD was supported by NSF Grant No. PHY 02-44653 while the theoretical calculations were supported in part by a grant from the Natural Science and Engineering Research Council of Canada.

[1] S. J. Gilbert, C. Kurz, R. G. Greaves, and C. M. Surko, Appl. Phys. Lett. **70**, 1944 (1997).
[2] S. J. Gilbert, R. G. Greaves, and C. M. Surko, Phys. Rev. Lett. **82**, 5032 (1999).
[3] J. P. Sullivan, S. J. Gilbert, J. P. Marler, R. G. Greaves, S. J. Buckman, and C. M. Surko, Phys. Rev. A **66**, 042708 (2002).
[4] W. E. Kaupilla, C. K. Kwan, D. Przybyla, S. J. Smith, and T. S. Stein, Can. J. Phys. **74**, 474 (1996).
[5] C. Kurz, S. J. Gilbert, R. G. Greaves, and C. M. Surko, Nucl. Instrum. Methods Phys. Res. B **143**, 188 (1998).
[6] R. P. McEachran, A. D. Stauffer, and L. E. M. Campbell, J. Phys. B **13**, 1281 (1980).
[7] I. P. Grant, B. J. McKenzie, P. Norrington, D. Mayers, and N. Pyper, Comput. Phys. Commun. **21**, 207 (1980).
[8] D. F. Register, L. Vuskovic, and S. Trajmar, J. Phys. B **19**, 1685 (1986).
[9] R. P. McEachran and A. D. Stauffer, J. Phys. B **20**, 3483 (1987).